Perspectives in Communication, Embedded-Systems and Signal-Processing (PiCES)
ISSN: 2566-932X, Vol. 2, Issue 12, March 2019
Proceedings of National Conference on Emerging Trends in VLSI, Embedded and Networking (NC-EVEN 18), April 2018

Design and Performance Analysis of a New Multiresolution M-ary Differential Chaos Shift Keying Communication System

Chetan Kalyani

Student, B.E, Department of Electronics and Communication, M.S.Engineering College, Bengaluru, Karnataka, India.
Chetankalyani96@gmail.com

Abstract - A new multiresolution (MR) M-ary differential chaos shift keying (DCSK) modulation scheme is proposed in this paper. It is a promising technique to provide different quality of services (QoS) for transmitted bits within a symbol according to their different bit error rate (BER) requirements based on the principle of non-uniformly spaced constellations. The new system not only is simple, but also provides better anti-multipath fading performance against various spreading factors, which inherits the advantages of the conventional DCSK system. Furthermore, the proposed scheme and its multicarrier version further increase spectral efficiency and use lower energy consumption at the same bandwidth as compared to the conventional DCSK and its multicarrier (MC- DCSK) system. Explicit BER expressions of the new system are derived and analysed over additive whiteGaussian noise (AWGN) aswell as multipath Rayleigh fading channels .All simulation results verify the prominent advantages of the new scheme and the accuracy of the new analytical approach.

Keywords— Multiresolution; M-ary DCSK; BER; AWGN channel; Multipath Rayleigh fading channel

I. INTRODUCTION

Conventional multiresolution (MR) modulation such as phase shift keying (PSK) and quadrature amplitude modulation (QAM) is a promising technique providing different quality of services (QoS) for transmitted bits according to their levels of importance. One advantage of the MR modulation is that it can support unequal error protection, i.e., a bit stream can be separated into several sub-streams with different levels of priority, including a high priority (HP) sub-stream and some lower priority (LP) sub-streams. The HP and LP data can be multiplexed and transmitted using an MR modulation in multimedia transmission digital broad-cast simultaneous voice and multiclass data transmissions cooperative and relay systems and user scheduling in cellular networks. Another advantage is that it does not extend the bandwidth as compared to channel coding techniques which add redundancy into the transmitted data.

The reason for applying the multiresolution technique to chaos-based modulations lies in the significant advantages provided by chaotic signals. A chaotic signal has a unique characteristic of being sensitive to initial conditions, which allows the generation of a theoretically infinite number of uncorrelated signals. Owing to their wideband characteristics, chaotic signals have proven to be one of the natural candidates for spread-spectrum modulation schemes. Hence, chaos-based modulation is a kind of combining modulation with spread spectrum technology which has similar advantages as conventional spread-spectrum modulations, e.g. mitigation of fading channels, anti-jamming and low probability of interception (LPI) and secure communications. In addition, chaos-based sequences outperform Gold sequences in spread-spectrum communication systems.

The novel contributions of this are summarized as follows

1) A new multiresolution M-ary DCSK system is designed. It provides different QoS for transmitted bits within a symbol according to their different BER requirements.
2) In addition to the advantages of the conventional DCSK and MC-DCSK systems, the new system and its multi-carrier version further increase the spectral efficiency and energy efficiency with the same bandwidth.
3) The analytical BER expressions of the proposed scheme over AWGN and multipath Rayleigh fading channels are derived and analysed

II. M-ARY DCSK SYSTEM

In this chapter, we present the M-ary DCSK system, which is an extension of the 4-ary DCSK system, and then give the BER performance by simulations over AWGN channels.

A. Principle of DCSK System

The system based on M-ary DCSK modulation is shown in Fig. 1. First, the chaotic generator generates a chaotic reference signal c_x, which is transformed into another quadrature signal c_y by using

Conference held at Brindavan College of Engineering, Yelahanka, Bagalur Main Rd, Dwarka Nagar, Bengaluru - 560063

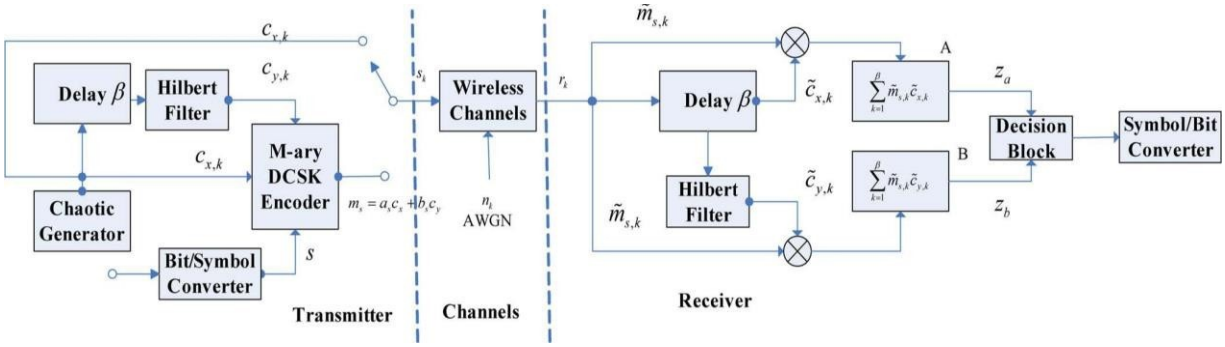

Fig 1. Block diagram of the M-ary DCSK scheme

Hilbert transform, thus two independent orthogonal chaotic signals are generated. For M-ary DCSK encoder (for the information signal), a constellation of chaotic signals can be generated as a linear combination of the quadrature signals c_x and c_y, in the form of $ms=a_sc_x+b_sc_y$, where the index s identifies the symbol in the signal space with s =1. . … M, and as and b_s present the real part and the image part corresponding to this symbol s, respectively(see Fig. 2 for 16-ary DCSK). Similarly, to DCSK, in the first half symbol period the reference signal cx is transmitted and in the second half symbol period the information-bearing signal $ms=a_sc_x+b_sc_y$ is sent. Hence, during the l-th symbol duration, the output of the transmitter is

$$s_k = \begin{cases} \sqrt{\frac{E_s}{2}} c_{x,k}, k = 2(l-1)\beta + 1, \ldots, 2(l-1)\beta + \beta \\ \sqrt{\frac{E_s}{2}} \left(a_s c_{x,k-\beta.} + b_s c_{y,k-\beta}\right), k = (2l-1)\beta + 1, \\ \ldots, 2l\beta \end{cases}$$

Where E_s is denoted by symbol energy, $\sum_{k=1}^{\beta} c_{x,k}c_{y,k}=0$, $\sum_{k=1}^{\beta} c^2_{x,k} = \sum_{k=1}^{\beta} c^2_{y,k}=1$, $a^2_x+b^2_s=1$ and 2β is a spreading factor.

At the receiver, the noise-corrupted reference signal c_x correlates the corrupted information-bearing signal, thus an observation value is obtained. Another observation value is computed by the corrupted reference signal, which is calculated by using the signal after Hilbert transform, and using the signal finally, the received symbol can be decided by the observation variables and using the decision boundaries and the received bits are reconstructed by the symbol/bits converter.

B. Results

The simulated results are presented here to show the BER performance of M-ary DCSK modulation over AWGN channels. It was found in that for small spreading factors β < 16, DCSK performs slightly better than 4-ary DCSK, while for large spreading factors, 4-ary DCSKoutperforms DCSK. Hence, a large spreading factor is adopted in the simulation. On the other hand, the logistic map xk+1= 1 − 2x2k is used as the chaotic system. For the normalized chaotic signal with zero mean, the variance is equal to one.

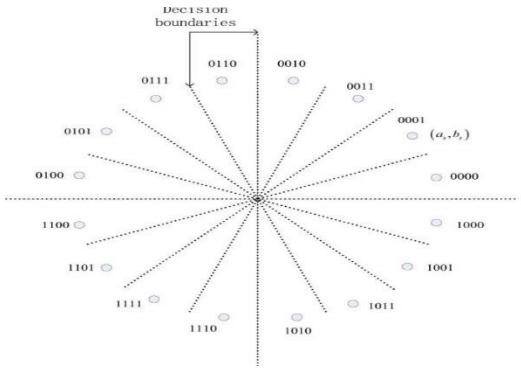

Fig 2. 16-ary DCSK constellation and its Gray coded mapping and decision boundaries.

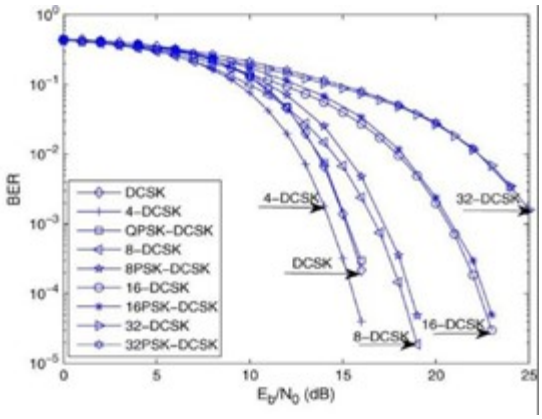

Fig 3. The BER performance curves of M-ary DCSK and MPSK-DCSK for spreading factor β=60 and M = 2, 4, 8, 16, and 32.

Fig. 3 shows the BER performance curves of M-ary DCSK and MPSK-DCSK for spreading factor β= 60 and M= 2, 4, 8, 16, and 32, respectively. For these two systems, it is observed that as the order M becomes higher than 4, the BER performance decreases with an increase of the order. The best BER performance of

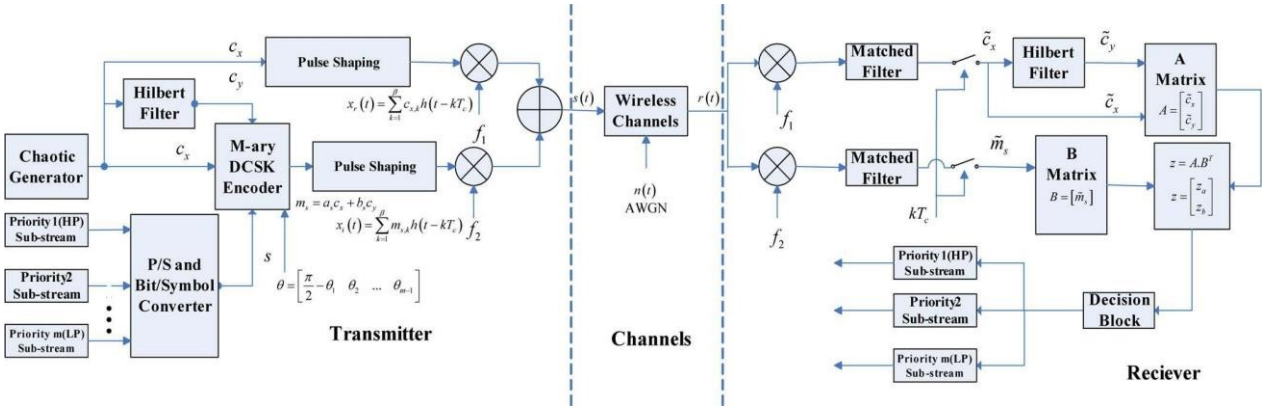

Fig 4. Block diagram of the MR M-ary DCSK scheme.

4-ary DCSK is obtained, which is different from the MPSK-DCSK system where PSK-DCSK and QPSK-DCSK have the same BER performance. Moreover, it is observed that the performance of M-ary DCSK is a little better than that of MPSK-DCSK, especially at a low order, M= 4 and 8. Finally, a better performance of the M-ary DCSK system is gained at the cost of a slightly higher complexity where the Hilbert transform operation is performed twice, as compared to the MPSK-DCSK system.

III. MULTIRESOLUTION M-ARY DCSK SYSTEM

In the case of MR 8-ary DCSK, the binary DCSK constellation represents the highest priority, which is represented by the "*" symbol. The 4-ary DCSK constellation, i.e., the angle $\pi/2 - \theta_1$ ($\theta_1 \leq \pi/4$, if the angle $\theta_1$is larger than $\pi/4$, the information of the position is the HP bit) represents the second priority, denoted by the" "symbol. The angle θ_2 denotes the third priority, which is marked by the "◦" symbol. Therefore, the binary DCSK modulation has the highest priority followed by 4- ary and 8-ary DCSK modulations. In other words, its principle is the same as the hierarchical PSK modulation. In Fig. 5, the MR 8-ary DCSK constellation also evolves from 4-ary DCSK modulation, which evolves from a binary DCSK modulation. Thus, we also refer this MR 8-ary DCSK constellation to as 2/4/8-ary DCSK, similarly to the hierarchical PSK modulation. In addition, it is noted that the "*" symbols are only fictitious symbols, while the actual transmitted symbols are the "◦" symbols.

A. The Transmitter

In this system, the parallel information sequences of different QoS or different kinds of data services are first converted into a k-bit serial sequence by a parallel-to-serial converter, which is converted into a symbol s by using a bits/symbol converter. The symbol s is encoded into the information signal by the M-ary DCSK encoder, i.e. $m_s=a_sc_x+b_sc_y$, where a_s and b_s are generated by the angle vector θ. Finally, the chaotic reference signal and information signals $x_r(t) = \sqrt{E_s/2\sum_{k=1}^{\beta} c_{x,k}}h(t-kT_c)$ and $x_i(t)=\sqrt{E_s/2\sum_{k=1}^{\beta} m_{s,|k}}h(t-kT_c)$, respectively are generated by pulse shaping, where h (t)is the square-root-raised-cosine filter and T_c is the chip time.

The transmitted signal of the MR M-ary DCSK can be expressed as

$$s(t) = x_r(t)\cos(2\pi f_1 t + \phi_1) + x_i(t)\cos(2\pi f_2 t + \phi_2) \quad (1)$$

where ϕ_1 and ϕ_2 denotes the phase angles of the carrier modulation. And the two modulated carries are orthogonal.

B. The Receiver

The received signal is given by

$$r(t) = \sum_{l=1}^{L} \alpha_l \delta(t-\tau_l) \otimes s(t) + n(t), \quad (2)$$

Where L is the number of paths, 1 and τ is the channel coefficient and the path delay of the l-th path, respectively, ⊗is the convolution operator, and n (t) is a wideband AWGN with zero mean and power spectral density of $N_0/2$. Assume that α_1 are independent Rayleigh distribution random variables. If the number of paths is equal to one, i.e. L = 1, with a unit channel coefficient α_1= 1, then this is the AWGN case; otherwise, the Rayleigh fading case. This multipath Rayleigh fading channel model is commonly used in spread- spectrum wireless communication systems. To simplify the analysis. we only discuss L independent and identically-distributed .Rayleigh fading channels, i.e. E $[|\alpha_1|^2]$ = E $[|\alpha_2|^2]$ = . . . = E $[|\alpha_L|^2]$, while similar results are obtained for other cases. Thus, the probability density function (PDF) of the symbol-SNR γ_s can be written as

$$f(\gamma_s) = \frac{\gamma_s^{L-1}}{(L-1)!\overline{\gamma}_c^{L}} \exp\left(-\frac{\gamma_s}{\overline{\gamma}_c}\right), \quad (3)$$

where $\overline{\gamma}_c$ is the average symbol-SNR per channel defined by

$$\overline{\gamma}_c = (E_s/N_0)E[\alpha_j^2] = (E_s/N_0)E[\alpha_l^2], j \neq l, \quad (4)$$

and

$$\gamma_s = \left(\sum_{l=1}^{L} \alpha_l^2\right) \frac{E_s}{N_0}, \quad (5)$$

with $\sum_{l=1}^{L} E[\alpha_l{}^2]=1$

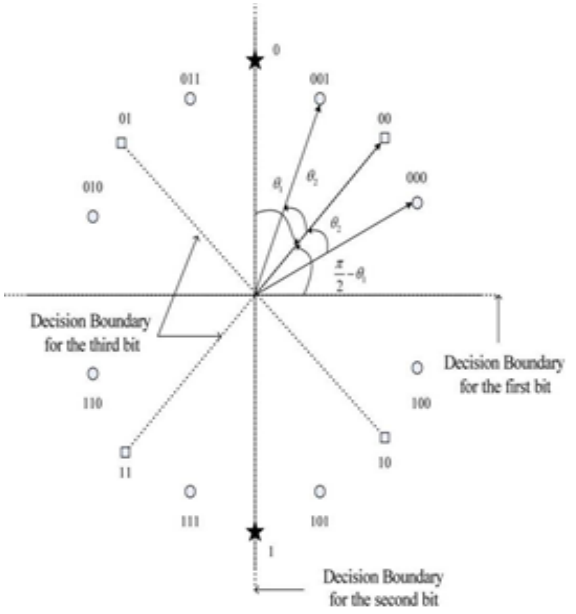

Fig 5. Generalized MR 8-ary DCSK constellation and its Gray coded map-ping and decision boundaries

The received signal r (t) is firstly separated by two corresponding modulated carrier frequencies. The separated signals are filtered by two corresponding matched filters. Then, the two filtered signals are sampled every KT_c time unit. This way, the desired Signals are demodulated. The desired reference signals and the signals after their Hilbert transforms are stored in matrix A. The desired information signals are stored in matrix B. Finally, the matrix product $z = A \times B^T$ is computed, thus the decision vector (z_a, z_b) is obtained.

C. Decisions

The decision vector is reconverted into the phase $\omega=\arctan(z_b/z_a)$. This phase is then adopted for decoding the bit streams, i.e. identifying the most likely transmitted phase θ, so that one can get the information bits corresponding to this θ. The decision method is different from the M-ary DCSK, where individual bits instead of symbols are decoded. For example, in the case of MR 8-ary DCSK, shown in Fig. 5, the HP bit is "0" if the received phase is $0 < \omega < \pi$; otherwise bit "1" is identified. Similarly, the second priority bit is "0" in the right half plane; otherwise, it is "1". However, the LP bits can be determined by the decision boundaries for which a computing method was given in [4]. For m≥ 3, the decision boundaries are necessary to calculate. Hence, the angle vector is known at the receiver.

IV. PERFORMANCE ANALYSIS OF MR M- ARY DCSK

A. Derivation of the CDF

The decision variables at the output of the correlators may be approximated as, respectively

$$z_a \approx \sum_{k=1}^{\beta} \left[\left(\sum_{l=1}^{L} \sqrt{\frac{E_s}{2}} \alpha_l c_{x,k-\tau_l} + n_k \right) \times \left(\sum_{l=1}^{L} \sqrt{\frac{E_s}{2}} \alpha_l \left(a_s c_{x,k-\tau_l} + b_s c_{y,k-\tau_l} \right) + n_{k+\beta} \right) \right], \quad (6)$$

$$z_b \approx \sum_{k=1}^{\beta} \left[\left(\sum_{l=1}^{L} \sqrt{\frac{E_s}{2}} \alpha_l c_{y,k-\tau_l} + \overline{n}_k \right) \times \left(\sum_{l=1}^{L} \sqrt{\frac{E_s}{2}} \alpha_l \left(a_s c_{x,k-\tau_l} + b_s c_{y,k-\tau_l} \right) + n_{k+\beta} \right) \right], \quad (7)$$

The variances of (6) and (7) are computed as respectively.

$$Var[z_a] = \sum_{l=1}^{L} \alpha_l^2 \frac{E_s N_0}{2} + \frac{\beta N_0^2}{4},$$

$$Var[z_b] = \sum_{l=1}^{L} \alpha_l^2 \frac{E_s N_0}{2} + \frac{\beta N_0^2}{4},$$

Where n_k is an AWGN with zero mean and variance $N_0/2$, and n_k is the Hilbert transform of $\overline{n_k}$, which is also an AWGN with zero mean and variance $N_0/2$.

It can be seen that the decision variables z_a and z_b are independent Gaussian variables with means $m_1 = \sum_{l=1}^{L} a_s \propto_1{}^2 \frac{E_s}{2}$ and $m_2 = \sum_{l=1}^{L} b_s \propto_1{}^2 \frac{E_s}{2}$ respectively, and with the same variance $\delta^2 = \sum_{l=1}^{L} \propto_1{}^2 \frac{E_s+N_0}{2} + \frac{\beta N_0{}^2}{4}$. Hence, the instance PDF is given by

$$p(z_a, z_b) = \frac{1}{2\pi\delta^2} \exp\left(-\frac{(z_a - m_1)^2 + (z_b - m_2)^2}{2\delta^2} \right)$$

Next, introduce the polar coordinates transformations of the decision vector (Z_a, Z_b) by

$$\begin{cases} V = \sqrt{z_a^2 + z_b^2} \\ \Omega = \arctan\left(\frac{z_b}{z_a}\right) \end{cases}$$

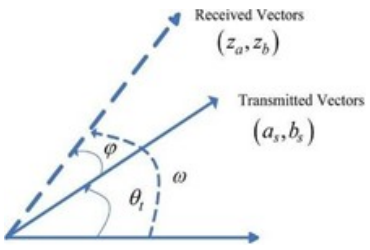

Fig 6. Signal vector perturbed by noise.

The cumulative distribution function (CDF) is given by

$$F(\phi) = \int_{-\pi}^{\phi} p(\varphi)d\varphi, -\pi < \phi < \pi$$

The CDF has the following characteristics:

$$\begin{cases} F(-\pi) = 0, F(\pi) = 1, F(0) = 1/2 \\ p(\varphi) = p(-\varphi) \end{cases}$$

V. NUMERICAL RESULTS AND DISCUSSIONS

A. BER Comparisons with Conventional DCSK, M-ary DCSK and MC-DCSK

This is used to compare BER performance among the MR M-ary DCSK, conventional DCSK, and M- ary DCSK (including 4-ary DCSK). The spreading factor β is set to 160 and the priority vector is set to θ= [π/3.5π/15π/40].

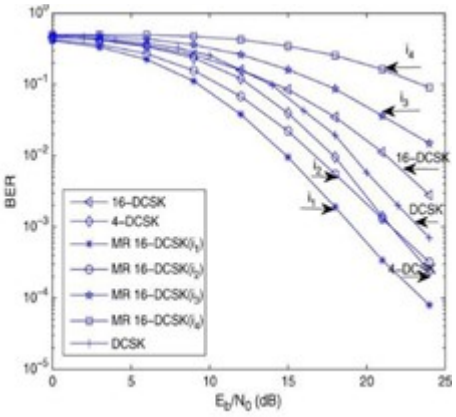

Fig 7. BER performance comparisons between MR 16-ary DCSK with priority vectors θ= [π/3.5 π/15 π/40], DCSK, 4-ary DCSK and 16-ary DCSK for spreading factor β= 160 over multipath Rayleigh fading channels.

Fig.8 shows the BER performance comparisons among the MR 16-ary DCSK, conventional DCSK, 4-ary DCSK and 16-aryDCSKovermultipath Rayleigh fading channels .It is observed that with the same bandwidth the transmission rate of the MR 16-ary DCSK system is four times than that of the DCSK system and it ensures that two bits be transmitted reliably as compared with the DCSK system. In addition, compared to the 4-ary DCSK, the MR16-ary DCSK obtains better performance at average BER of the high and second priority data and also increases the transmission rate. Furthermore, compared with the16-ary DCSK ,the MR16-ary DCSK can provide different reliability requirements.

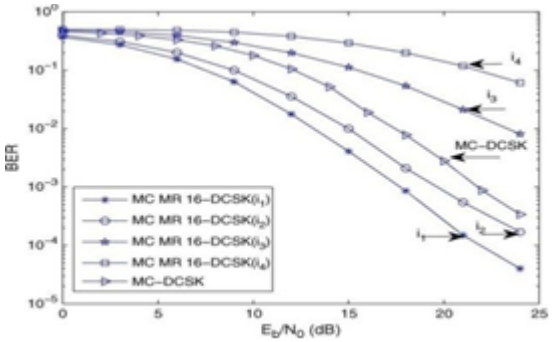

Fig 8. BER performance comparisons between MC MR 16-ary DCSK with priority vectors θ= [π/3.5 π/15 π/40] and MC-DCSK for spreading factor β=160 over multipath Rayleigh fading channels

To compare with the MC-DCSK, the proposed scheme is extended into the MC system. Here, the number of subcarriers is set to 4, the spreading factor β is set to 160 and the priority vector is set to θ= [π/3.5 π/15 π/40]. Fig. 9 shows the BER performance comparisons between the MC MR 16- ary DCSK and MC-DCSK over multipath Rayleigh fading channels. From the curves, it can be seen that, the proposed scheme offers higher data rate and lower energy consumption with the same bandwidth. In addition, every subcarrier can be equipped with different MR M-ary DCSK according to different requirements.

VI. CONCLUSION

A new simple generalized multiresolution M-ary DCSK system is designed. The new system enables simultaneous transmission of multiple sub-streams of the original stream with different levels of priority through the use of non-uniformly spaced constellations. Moreover, it offers better anti- multipath fading performance due to various spreading factors which inherits the advantages of the conventional DCSK system analytical BER expressions of the proposed system are derived over AWGN as well as multipath Rayleigh fading channels. Simulation results well match the analytical BER expressions, which demonstrate the accuracy of the proposed analytical method. These analytical BER expressions are de-pendent on the constellation size, the SNR, the spreading factors which ensure anti-multipath fading performance, and a constellation parameter which controls the relative message importance. Through adjusting the constellation parameter, the BER performance of different data priorities satisfies different service requirements without extending the bandwidth, which is different from channel coding. Compared to the DCSK and MC-DCSK, the proposed scheme and its multicarrier version further increase the spectral efficiency and energy efficiency with the same bandwidth.

REFERENCES

[1] T. Cover, "Broadcast channels," IEEE Trans. Info. Theory, vol. IT-18, no. 1, pp. 2-14, Jan. 1972.

[2] K. Ramchandran, A. Ortega, K.M. Uz, and M.Vetterli, "Multiresolution broadcast for digital HDTV using joint source/channel coding," IEEE J. Select. Areas Commun, vol. 11, no. 1, pp. 6-23, Jan. 1993.

[3] L. Wei, "Coded modulation with unequal error protection," IEEE Trans. Commun., vol. 41, no. 10, pp. 1439-1449, Oct. 1993.

[4] P. Vitthaladevuni and M. Alouini, "Exact BER computation of generalized hierarchical PSK constellations," IEEE Trans. Commun., vol. 51, no. 12, pp. 2030-2037, Dec. 2003.

[5] P. Vittahaladevuni and M. S. Alouini, "A recursive algorithm for the exact BER computation of generalized hierarchical QAM constellations," IEEE Trans. Info. Theory, vol. 49, no. 1, pp. 297-307, Jan. 2003.

[6] M. Pursley and J. Shea, "Adaptive nonuniform phases-shift- key modulation for multimedia traffic in wireless networks," IEEE J. Sel. Areas Commun., vol. 18, no. 8, pp. 1394-1407, Aug. 2000.

[7] D T. V. Nguyen, P. C. Cosman, and L. B. Milstein, "Double-layer video transmission over decode-and-forward wireless relay networks using hierarchical modulation," IEEE Trans. Image Processing, vol. 23, no. 4, pp. 1791-1804, Apr. 2014.

[8] H. Choi, I. Shin, J. Lim, and J. Hong, "SVC application in advanced T-DMB," IEEE Trans. Broadcast., vol. 55, no. 1, pp. 51-61, Mar. 2009.

[9] ETSI, Framing Structure, Channel Coding and Modulation for Satellite Services to Handheld Devices (SH) Below 3 GHz. ETSI EN 302 583 V1.1.1 (2008-03), Digital Video Broadcasting (DVB), 2008.

[10] H. Jiang and P. A. Wilford, "A hierarchical modulation for upgradingdigital broadcast systems," IEEE Trans. Broadcast., vol. 51, no. 2, pp. 223229, Jun. 2005.

[11] H. Jiang, P. A. Wilford, and S. A. Wilkus, "Providing local content in a hybrid single frequency network using hierarchical modulation," IEEE Trans. Broadcast., vol. 56, no. 4, pp. 532-540, Dec. 2010.

[12] Md. J. Hossain, P. Vitthaladevuni, M.-S. Alouini, V. K. Bhargava, and A. Goldsmith, "Adaptive hierarchical modulation for simultaneous voice and multiclass data transmission over fading channels," IEEE Trans. Veh. Technol., vol. 55, no. 4, pp. 1181-1194, Jul. 2006.

[13] E. G. Larsson and B. R. Vojcic, "Cooperative transmit diversity based on superposition modulation," IEEE Commun. Lett., vol. 9, no. 9, pp. 778-780, Sept. 2005.

[14] M. K. Chang S. Y. Lee, "Performance Analysis of Cooperative Communication System with Hierarchical Modulation over Rayleigh Fading Channel," IEEE Trans. Wireless Commun., vol. 8, no. 6, pp. 2848-2852, Jun. 2009.

[15] C. Hausl and J. Hagenauer, "Relay communication with hierarchical modulation," IEEE Commun. Lett., vol. 11, no. 1, pp. 64-66, Jan. 2007.

[16] J. Park, S. Kim, and J. Choi, "Hierarchical modulated network coding for asymmetric two-way relay systems," IEEE Trans. Veh. Technol., vol. 59, no. 5, pp. 2179-2184, Jun. 2010.

[17] Md. J. Hossain, M.-S. Alouini, and V. K. Bhargava, "Multi-user opportunistic scheduling using power controlled hierarchical constellations," IEEE Trans. Wireless Commun., vol. 6, no. 5, pp. 1581-1586, May 2007.

[18] Md. J. Hossain, M.-S. Alouini, and V. K. Bhargava, "Rate adaptive hierarchical modulation-assisted two-user opportunistic scheduling," IEEE Trans. Wireless Commun., vol. 6, no. 6, pp. 2076-2085, Jun. 2007.

[19] Md. J. Hossain, M.-S. Alouini, and V. K. Bhargava, "Two- user opportunistic scheduling using hierarchical modulations in wireless networks with heterogenous average link gains," IEEE Trans. Commun., vol. 58, no. 3, pp. 880-889, Mar. 2010.

[20] Q. Li, J. Zhang, L. Bai, J. Choi, "Performance analysis and system design for hierarchical modulated BICM-ID," IEEE Trans. Wireless Commun., vol. 13, no. 6, pp. 3056-3069, Jun. 2014

[21] F. C. M. Lau and C. K. Tse, Chaos-Based Digital communication systems. Springer-Verlag, 2003.

[22] L. Ye, G. Chen, L. Wang, "Essence and advantages of FM- DCSK technique versus conventional spreading spectrum communication method," Circuits, Systems and Signal Processing, vol. 24, no. 5, pp. 657-673, Oct. 2005.

[23] J. Yu and Y. Yao, "Detection performance of chaotic spreading LPI waveforms," IEEE Trans. Wireless Commun., vol. 4, no. 2, pp. 390-396, Mar. 2005.

[24] G. Mazzini, G. Setti, and R. Rovatti, "Chaotic complex spreading sequences for asynchronous DS-CDMA Part I: system modelling and results," IEEE Trans. Circuits Syst.-I, vol. 44, no. 10, pp. 937-1947, Oct. 1997.

[25] A. P. Kurian, S. Puthusserypady, and S. M. Htut, "Performance enhancement of DS/CDMA system using chaotic complex spreading sequence," IEEE Trans. Wireless Commun., vol. 4, no. 3, pp. 984-989, May 2005.

[26] H. Dedieu, M. P. Kennedy, M. Hasler, "Chaos shift keying: modulation and demodulation of a chaotic carrier using self-synchronising Chua's circuits," IEEE Trans. Circuits Syst.- II, vol. 40, no. 10, pp. 634-642, Oct. 1993.

[27] G. Kolumban, B. Vizvari, W. Schwarz, A. Abel, "Differential chaos shift keying: A robust coding for chaos communications," in Proc. Int. Workshop Nonlinear Dyn. Electron. Syst., Seville, Spain, Jun. 1996, pp. 87-92.